**Heat and Technology**
Vol. 32, n. 1-2, 2014

# CONVECTIVE HEAT AND MASS TRANSFER IN AN MHD NANO FLUID IN THE PRESENCE OF CHEMICAL REACTION AND THERMAL RADIATION

*S. O Bello, **B. I Olajuwon and ***S. I Kuye

*Department of Mathematics and Statistics, Federal Polytechnic Ilaro,Ilaro, Nigeria.
**Department of Mathematics, Federal University of Agriculture, Abeokuta, Nigeria.
**Corresponding email: olajuwonishola@yahoo.com
***Department of Mechanical Engineering,Federal University of Agriculture, Abeokuta, Nigeria.

***ABSTRACT***

*This paper examined the effect of chemical reaction and thermal radiation on the heat and mass transfer in an MHD water based nanofluid over a vertical plate. The nanoparticles used in this study were of Copper (Cu), Silver (Ag), Alumina ($Al_2O_3$) and Titanium Oxide ($TiO_2$). The momentum, energy and concentration species equations governing the flow, heat and mass transfer were reduced to a set of ordinary differential equations by using the appropriate similarity transformations for the velocity components, temperature and concentration. These equations were then solved numerically by employing the Runge-Kutta-Fehlberg shooting techniques. The effects of pertinent parameters such as; chemical reaction, thermal radiation, magnetic field, Schmidt number, particle volume fractions and the Prandtl number on the heat and mass transfer were studied. By using different types of nanofluid, the results indicate that the parameters studied have influence on the flow, heat and mass transfer in an MHD nanofluid.*

**Keywords:** *chemical reaction, thermal radiation, heat andmass transfer, magnetic field,, water based nanofluid, particle volume fractions*

**INTRODUCTION:-** A wide variety of industrial processes involve the transfer of heat energy because throughout any industrial facility, heat must be added, removed or moved from one process stream to another and this has become a major task for industrial necessity. These processes provide a source for energy recovery and process fluid heating/cooling.

The discovery of nanofluids is very recent and many researchers have studied and written much about heat and mass transfer in nanofluids. Most authors have concerned themselves on its preparation and characteristics while a few have looked into its behaviour, effectiveness and applications.

Alloui et al [1] made an analytical and numerical study of bouyancy-driven convection in a vertical enclosure filled with nanofluids. Using three models to simulate the effective dynamic viscosity $\phi$ of the nanofluids, they asserted that the parameter affects the convective heat transfer performance of the nanofluids confined inside the enclosures.Fakhreddine and Bennaccer [2] investigated the convective heat transfer using different nanofluid types where the nanofluids are treated as heterogeneous mixtures with weak solutal diffusivity and possible Soret separation. Godson et al [3] and Ozerinc et al [9], in separate papers, agreed that Nanofluids are, recently, the most intensively investigated option to enhance heat transfer and showed that a very small amount of nanoparticles dispersed uniformly and suspended stably in base fluids can provide impressive improvement in the thermal property of such fluids.Hamad, [4] found the analytical solution to the problem of natural convection flow of a nanofluid over a linearly stretching sheet in the presence of a magnetic field. He concluded that nanofluids will be important in the cooling and heating processes. This is because the shear stress and the rate of heat transfer change with different types of nanofluids.Kakac and Pramuanjaroenkij[5] presented a summaryof the recent progress on the study of nanofluids, such as thepreparation methods, the evaluation methods for the stability of nanofluids, and the ways to enhance the stability for nanofluids.Khan and Pop [6] examined the boundary-layer flow of a nanofluid past a stretching sheet.Kuznetsov and Neid [7] studied the convective heat transfer in a nanofluid past a vertical plate using a model which accounted for the Brownian motion and thermophoresis with simplest possible boundary conditions, namely those in which both the temperature and the nanoparticle fraction are constant along the wall.Hyun and Jang [8] examined the effect of nanofluids on the thermal performance of a flat micro heat pipe with rectangular grooved wick. The outcome of their examination is that, the thin porous coating layer formed by nanoparticles suspended in nanofluid is a key effect of the heat transfer enhancement for the heat pipe using nanofluids.Sarmaet. al [10] developed a model based on the available experimental data for nano-particles inclusion of $Al_2O_3$ and Cu in the base medium of water to predict eddy momentum diffusivity and eddy thermal diffusivity. Sarmaet. Al [11] presented an experimental investigation d with $Al_2O_3$nanofluid of 47nm size at different volumetric concentrations to establish correlations for Nusselt number and friction factor in the turbulent range of Reynolds number. Wang and Mujumdar [12] recently reviewed the heat transfer characteristics of nanofluids. The team enumerated various methods of preparing nanofluids and pointed out few of their uses.

Sidiet. al [13] considered the problem oflaminar forced convection flow of nanofluids for two particular geometrical configurations, namely a uniformly heated tube and a system of parallel, coaxial and heated disks. They obtained numerical results for water–$\gamma Al_2O_3$ and Ethylene Glycol–$\gamma Al_2O_3$ mixtures

and the results showed that the inclusion of nanoparticles into the base fluids produced a considerable augmentation of the heat transfer coefficient that clearly increases with an increase of the particle concentration. Khairyet, al [14], presented the numerical study of the steady boundary layer flow and heat transfer of a nanofluid past a nonlinearly permeable stretching/shrinking sheet. They showed that dual solutions exist in a certain range of the stretching/shrinking parameter for both shrinking and stretching cases. Their results indicated that suction widens the range of the stretching/shrinking parameter for which the solution exists.Khanet. al [15] examined a two-dimensional steady flow of an electrically conducting, viscous incompressible nanofluid past a continuously moving surface in the presence of uniformtransverse magnetic field with chemical reaction. Rasekh et al. [16] have analyzed the flowand heat transfer of nanofluids over a stretching cylinder. And their result show that the thermophoresis and Brownianmotion forces have significant effect on the heat transfer rate of nanofluids inthe boundary layer. Aminreza et. al [17 ] presented the development of the steady boundary layer flow and heattransfer of a magnetohydrodynamicnanofluid over astretching cylinder. And the result showed that increase in the magnetic parameter caused decrease in the magnitude of velocity profiles, but it increases the magnitude of temperatureand concentration profiles in the boundary layer.
In this paper, we shall extend previous works and investigate the convective, heat and mass transfer in a water based nanofluid, with various nanoparticles volume ratios, under the influence of a magnetic field in the presence of both thermal radiation and the chemical reaction.

## 2.1 MATHEMATICAL FORMULATION

Consider the steady laminar two-dimensional flow of an incompressible viscous nanofluid past a linearly semi-infinite stretching sheet under the influence of a constant magnetic field of strength $\beta_0$ which is applied normally to the sheet. A water based nanofluid containing different types of nanoparticles: $Al_2O_3$, Cu, $TiO_2$ and Ag is used with the assumption that both the fluid and the nanoparticles are in thermal equilibrium. The $\bar{x}$ - direction is taken along the plate in the upward direction and $\bar{y}$ -axis is taken normal to it as shown in fig. 2.

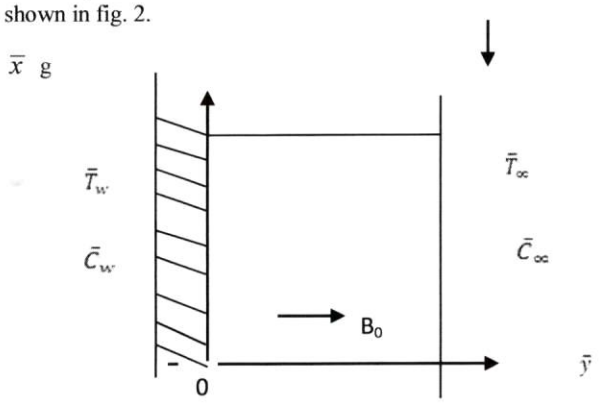


**Fig 1: Physical model**

We shall also assume that no slip occurs between them. Hence, the governing boundary layer equations of continuity, momentum, thermal and concentration for the flow under the aforesaid assumptions are

$$\frac{\partial \bar{u}}{\partial \bar{x}} + \frac{\partial \bar{v}}{\partial \bar{y}} = 0 \tag{1}$$

$$\rho_{nf}\left(\bar{u}\frac{\partial \bar{u}}{\partial x} + \bar{v}\frac{\partial \bar{u}}{\partial \bar{y}}\right) = \mu_{nf}\frac{\partial^2 \bar{u}}{\partial \bar{y}^2} - \sigma\beta_0\bar{u} + g\lambda(\bar{T} - \bar{T}_\infty) + g\beta_0(\bar{\phi} - \bar{\phi}_\infty) \tag{2}$$

$$\left(\rho C_p\right)_{nf}\left(\bar{u}\frac{\partial \bar{T}}{\partial x} + \bar{v}\frac{\partial \bar{T}}{\partial \bar{y}}\right) = k_{nf}\frac{\partial^2 \bar{T}}{\partial \bar{y}^2} - \frac{\partial q_r}{\partial \bar{y}} \tag{3}$$

$$\left(\bar{u}\frac{\partial \bar{\phi}}{\partial x} + \bar{v}\frac{\partial \bar{\phi}}{\partial \bar{y}}\right) = D_m\frac{\partial^2 \bar{\phi}}{\partial \bar{y}^2} - R(\bar{\phi} - \bar{\phi}_\infty) \tag{4}$$

Where $q_r$ is the radiative heat flux, $D_m$ is the molecular difusivity, T is the temperature of the fluid, $\phi$ is the Concentration of the solute and R is rate of chemical reaction. $\bar{x}$ and $\bar{y}$ are the coordinates along and perpendicular to the sheet while $\bar{u}$ and $\bar{v}$ are the velocity components in the $\bar{x}$ and $\bar{y}$ directions respectively.

The boundary conditions of eqations (1) – (4) are

$$\bar{u} = \bar{u}_w(\bar{x}) = a\bar{x},\ \bar{v} = 0,\ \bar{T} = \bar{T}_w,\ \bar{\phi} = \bar{\phi}_w \text{ at } \bar{y} = 0$$

$$\bar{u} \to 0,\ \bar{T} \to \bar{T}_\infty,\ \bar{\phi} \to \bar{\phi}_\infty \text{ as } \bar{y} \to \infty \tag{5}$$

Where $a$ is a constant.

The effective density ($\rho_{nf}$), effective dynamic viscosity ($\mu_{nf}$), heat capacitance $(\rho C_p)_{nf}$ and the thermal conductivity ($k_{nf}$) of the nanofluid, in that order, are given as [12]

$$\left.\begin{aligned} \rho_{nf} &= (1 - A)\rho_f + A\rho_s\ ; \\ \mu_{nf} &= \frac{\mu_f}{(1 - A)^{2.5}} \\ (\rho C_p)_{nf} &= (1 - A)(\rho C_p)_f + A(\rho C_p)_s\ . \\ k_{nf} &= k_f\left\{\frac{k_s + 2k_f - 2A(k_f - k_s)}{k_s + 2k_f + 2A(k_f - k_s)}\right\} \end{aligned}\right\} \tag{6}$$

In these equations, A is the solid volume fraction ($A \neq 1$), $\mu_f$ is the dynamic viscosity of the base fluid, while $\rho_f$ and $\rho_s$ are the densities of the pure fluid and the nanoparticle respectively. The constants $k_f$ and $k_s$ are the thermal conductivities of the base fluid and the nanoparticle respectively.

Equations (1) – (4) can be made to be non-dimensional by the introduction of the following non-dimensional variables.

$$\left.\begin{aligned} u &= \frac{\bar{u}}{\sqrt{av_f}},\ v = \frac{\bar{v}}{\sqrt{av_f}},\ \theta = \frac{\bar{T} - \bar{T}_\infty}{\bar{T}_w - \bar{T}_\infty} \\ x &= \frac{\bar{x}}{\sqrt{v_f/a}},\ y = \frac{\bar{y}}{\sqrt{v_f/a}} \text{ and } \phi = \frac{\bar{\phi} - \bar{\phi}_\infty}{\bar{\phi}_w - \bar{\phi}_\infty} \end{aligned}\right\} \tag{7}$$

Following Rosseland approximation, the radiative heat flux $q_r$ is modelled as

$$q_r = \frac{-4\sigma^*}{3k^*}\frac{\partial \bar{T}^4}{\partial \bar{y}} \tag{8}$$

Where $\sigma^*$ = Stefen- Boltzman constant; $k^*$ = mean absorbtion coefficient.

Assuming that the difference in temperature within the flow are such that $\bar{T}^4$ can be expressed as a linear combination of the temperature using the Taylor's series expansion about $\bar{T}_\infty^4$ and neglecting higher order terms, then

$$\bar{T}^4 \approx -3\bar{T}_\infty^4 + 4\bar{T}_\infty^3\bar{T} \quad (9)$$

Differentiating equation (8) w.r.t. $\bar{y}$ and using (9), we obtain

$$\frac{\partial q_r}{\partial \bar{y}} = \frac{-16\sigma^*\bar{T}_\infty^3}{3k^*}\frac{\partial^2 \bar{T}}{\partial \bar{y}^2} \quad (10)$$

Substituting equation (10) into equation (3) and using equation (7) to transform equations (1) – (4), we have

$$\frac{\partial u}{\partial x} + \frac{\partial v}{\partial y} = 0 \quad (11)$$

$$u\frac{\partial u}{\partial x} + v\frac{\partial u}{\partial y} = \frac{1}{1 - A + A\rho_s/\rho_f}\left\{\frac{1}{(1-A)^{2.5}}\frac{\partial^2 u}{\partial y^2} - Mu + G_r\theta + G_r\phi\right\} \quad (12)$$

$$u\frac{\partial \theta}{\partial x} + v\frac{\partial \theta}{\partial y} = \frac{1}{p_r}\frac{1}{1 - A + A(\rho C_p)_s/(\rho C_p)_f}\left(\frac{k_{nf}}{k_f} + R\right)\frac{\partial^2 \theta}{\partial y^2} \quad (13)$$

$$u\frac{\partial \phi}{\partial x} + v\frac{\partial \phi}{\partial y} = \frac{1}{Sc}\frac{\partial^2 \phi}{\partial y^2} - \gamma\phi \quad (14)$$

Where, $Sc = \frac{\nu_f}{D_m}$ is the schmidth number ; $Pr = \frac{\nu_f}{k_f}$ is the Prandtl number;

$R = \frac{16\sigma^* T_\infty^3}{3k^* k_f}$ is the radiation parameter; $\gamma = \frac{R}{a}$ is the chemical reaction parameter

$G_r = \frac{g\beta_t(\bar{T}_w - \bar{T}_\infty)x}{a}$ is the Grashof number.

$G_c = \frac{g\beta_c(\bar{T}_w - \bar{T}_\infty)x}{a}$ is the modified Grashof number.

The boundary conditions (5) become

$u = x,\ v = 0,\ \phi = 1,\ \theta = 1$ at $y = 0$;

$u = 0,\ \phi = 0,\ \theta = 0$ as $y \to \infty$ (15)

## 2.2 SIMILARITY TRANSFORMATIONS

Equations (11) – (14) will now be transformed by introducing the stream function ψ, which is define as

$$u = \frac{\partial \psi}{\partial y}, \quad v = -\frac{\partial \psi}{\partial x}.$$

together with the similarity variable

$$\eta = y,\ \psi = xf(\eta),\ \theta = \theta(\eta)\ \phi = \phi(\eta)$$

to give

$$f''' + (1-A)^{2.5}\left\{ff'' - (f')^2\right\}(1 - A + A\rho_s/\rho_f)\} - (1-A)^{2.5}(Mf' + G_T\theta + G_C\phi) = 0 \quad (16)$$

$$\frac{1}{\Pr}\frac{1}{1 - A + A(\rho C_p)_s/(\rho C_p)_f}\left[\frac{k_{nf}}{k_f} + R\right]\theta''(\eta) + f(\eta)\theta'(\eta) = 0 \quad (17)$$

$$\phi''(\eta) + Scf(\eta)\phi'(\eta) - ScRc\phi(\eta) = 0 \quad (18)$$

The boundary conditions now become

$$f(0) = 0,\ f'(0) = 1 \text{ and } f' \to 0 \text{ as } \eta \to \infty \quad (19)$$

$$\theta(0) = 1,\ \theta(\infty) = 0 \text{ and } \phi(0) = 1\ \phi(\infty) = 0 \quad (20)$$

## 3.1 METHOD OF SOLUTION

The thermo physical properties of pure water and those of the nanoparticles as given in table 1 by [4] will now be substituted in the transformed three coupled ordinary differential equations, (16) - (18) involving the velocity, temperature and concentration of the nanofluidwith the boundary conditions (19) and (20) and then solved using Runge-Kutta-Fehlberg (RKF) method with shooting technique.

Table 1: Thermo physical properties of water and nanoparticles [4]

| Compound | ρ (kg/m$^3$) | $C_p$(J/kgK) | $k$ (W/mK |
|---|---|---|---|
| Pure water | 997.1 | 4179 | 0.613 |
| Copper (Cu) | 8933 | 385 | 401 |
| Alumina ($Al_2O_3$) | 3970 | 765 | 40 |
| Silver (Ag) | 10500 | 235 | 429 |
| Titanium Oxide ($TiO_2$) | 4250 | 686.2 | 8.9538 |

The results are shown in tables 2 – 7 and figures 2- 11

Table 2: Values of $-f''(0)$ for various M, A when $Gr = Gc = 0.1$, $Rc = 0.5$, $Sc = 0.62$ $Rd = 0.5$ and $\Pr = 6.2$:

| M | A | $-f''(0)$ | | | |
|---|---|---|---|---|---|
| | | $Cu$ | $Ag$ | $Al_2O_3$ | $TiO_2$ |
| 0 | 0.41 | 0.463799 | 0.464440 | 0.464035 | 0.464057 |
| | 0.45 | 0.429704 | 0.430310 | 0.429928 | 0.429954 |
| | 0.5 | 0.388153 | 0.388703 | 0.388357 | 0.388386 |
| | 0.6 | 0.308636 | 0.309047 | 0.308788 | 0.308815 |
| 2 | 0.41 | 0.852736 | 0.853325 | 0.852954 | 0.852974 |
| | 0.44 | 0.799491 | 0.800064 | 0.799703 | 0.799727 |
| | 0.45 | 0.781923 | 0.782490 | 0.782133 | 0.782158 |
| | 0.46 | 0.764449 | 0.765008 | 0.764656 | 0.764681 |
| 3 | 0.41 | 0.996169 | 0.996714 | 0.996371 | 0.996390 |
| | 0.45 | 0.912857 | 0.913388 | 0.913055 | 0.913078 |
| | 0.5 | 0.811081 | 0.811577 | 0.811265 | 0.811291 |
| | 0.53 | 0.751345 | 0.751814 | 0.751519 | 0.751546 |
| 6 | 0.41 | 1.339111 | 1.339545 | 1.339273 | 1.339288 |
| | 0.45 | 1.226547 | 1.226981 | 1.226710 | 1.226728 |
| | 0.58 | 0.876147 | 0.876516 | 0.876284 | 0.876308 |
| | 0.6 | 0.824554 | 0.824904 | 0.824684 | 0.824707 |

Table 3: Values of $-\theta'(0)$ for various Rd, A when $Gr = Gc = 0.1$, $Rc = 0.5$, $Sc = 0.62$ $M = 0.5$ and $\Pr = 6.2$:

| Rd | A | $-\phi'(0)$ | | | |
|---|---|---|---|---|---|
| | | $Cu$ | $Ag$ | $Al_2O_3$ | $TiO_2$ |
| 0 | 0.41 | 1.433536 | 1.350374 | 1.404143 | 1.408867 |
| | 0.45 | 1.438234 | 1.346403 | 1.405348 | 1.408884 |
| | 0.5 | 1.443657 | 1.340822 | 1.406356 | 1.408387 |
| | 0.6 | 1.452963 | 1.327525 | 1.406669 | 1.405619 |
| 2 | 0.41 | 0.972406 | 0.913413 | 0.949966 | 0.947921 |
| | 0.44 | 0.977543 | 0.913963 | 0.953262 | 0.950617 |
| | 0.45 | 0.979212 | 0.914093 | 0.954314 | 0.951468 |
| | 0.46 | 0.980860 | 0.914196 | 0.955343 | 0.952296 |
| 3 | 0.41 | 0.720683 | 0.674841 | 0.702753 | 0.699514 |
| | 0.45 | 0.728728 | 0.678139 | 0.708897 | 0.705050 |
| | 0.5 | 0.738269 | 0.681661 | 0.716038 | 0.711422 |
| | 0.53 | 0.743718 | 0.683450 | 0.720033 | 0.714950 |
| 6 | 0.41 | 0.438006 | 0.407237 | 0.425679 | 0.422606 |
| | 0.45 | 0.447406 | 0.413360 | 0.433771 | 0.430288 |
| | 0.58 | 0.475473 | 0.430550 | 0.457536 | 0.452693 |
| | 0.6 | 0.479435 | 0.432805 | 0.460829 | 0.455773 |

Table 4: Values of $-\phi'(0)$ for various M, A when $Gr = Gc = 0.1$, $Rc = 0.5$, $Sc = 0.62$ $Rd = 0.5$ and $\Pr = 6.2$:

| M | A | $-\phi'(0)$ | | | |
|---|---|---|---|---|---|
| | | $Cu$ | $Ag$ | $Al_2O_3$ | $TiO_2$ |
| 0 | 0.41 | 0.761097 | 0.761026 | 0.761071 | 0.761069 |
| | 0.45 | 0.765342 | 0.765275 | 0.765318 | 0.765315 |
| | 0.5 | 0.770617 | 0.770556 | 0.770595 | 0.770591 |
| | 0.6 | 0.781000 | 0.780955 | 0.780983 | 0.780980 |
| 2 | 0.41 | 0.725676 | 0.725600 | 0.725648 | 0.725646 |
| | 0.44 | 0.730404 | 0.730330 | 0.730377 | 0.730374 |
| | 0.45 | 0.732005 | 0.731932 | 0.731978 | 0.731975 |
| | 0.46 | 0.733618 | 0.733546 | 0.733591 | 0.733588 |
| 3 | 0.41 | 0.714699 | 0.714626 | 0.714672 | 0.714669 |
| | 0.45 | 0.721349 | 0.721279 | 0.721323 | 0.721320 |
| | 0.5 | 0.730060 | 0.729995 | 0.730036 | 0.730033 |
| | 0.53 | 0.735488 | 0.735428 | 0.735466 | 0.735463 |
| 6 | 0.41 | 0.692735 | 0.692673 | 0.692712 | 0.692710 |
| | 0.45 | 0.699639 | 0.699578 | 0.699617 | 0.699614 |
| | 0.58 | 0.725338 | 0.725289 | 0.725320 | 0.725317 |
| | 0.6 | 0.729738 | 0.729691 | 0.729721 | 0.729718 |

Table 5: Values of $-\phi'(0)$ for various Rd, A when $Gr = Gc = 0.1$, $Rc = 0.5$, $Sc = 0.62$ $\mathrm{M} = 0.5$ and $\Pr = 6.2$:

| Rd | A | $-\phi'(0)$ | | | |
|---|---|---|---|---|---|
| | | $Cu$ | $Ag$ | $Al_2O_3$ | $TiO_2$ |
| 0 | 0.41 | 0.749999 | 0.749955 | 0.749984 | 0.749987 |
| | 0.45 | 0.755056 | 0.755014 | 0.755042 | 0.755043 |
| | 0.5 | 0.761414 | 0.761376 | 0.761401 | 0.761402 |
| | 0.6 | 0.774123 | 0.774094 | 0.774113 | 0.774113 |
| 2 | 0.41 | 0.749638 | 0.749562 | 0.749610 | 0.749608 |
| | 0.44 | 0.753470 | 0.753398 | 0.753444 | 0.753441 |
| | 0.45 | 0.754751 | 0.754680 | 0.754725 | 0.754722 |
| | 0.46 | 0.756033 | 0.755963 | 0.756008 | 0.756005 |
| 3 | 0.41 | 0.749223 | 0.749114 | 0.749182 | 0.749174 |
| | 0.45 | 0.754404 | 0.754302 | 0.754366 | 0.754358 |
| | 0.5 | 0.760898 | 0.760808 | 0.760864 | 0.760857 |
| | 0.53 | 0.764792 | 0.764709 | 0.764761 | 0.764754 |
| 6 | 0.41 | 0.748223 | 0.748045 | 0.748154 | 0.748137 |
| | 0.45 | 0.753577 | 0.753414 | 0.753514 | 0.753497 |
| | 0.58 | 0.770844 | 0.770735 | 0.770803 | 0.770791 |
| | 0.6 | 0.773459 | 0.773358 | 0.773420 | 0.773410 |

Table 6: Values of $-\phi'(0)$ for various Sc, A when $Gr = Gc = 0.1$, $Rc = 0.5$, $Rd = 0.5$ $M = 0.5$ and $\Pr = 6.2$:

| Rc | A | $-\phi'(0)$ | | | |
|---|---|---|---|---|---|
| | | $Cu$ | $Ag$ | $Al_2O_3$ | $TiO_2$ |
| 0.1 | 0.41 | 0.553828 | 0.553755 | 0.553803 | 0.553807 |
| | 0.45 | 0.562821 | 0.562753 | 0.562798 | 0.562800 |
| | 0.5 | 0.573895 | 0.573835 | 0.573874 | 0.573875 |
| | 0.6 | 0.595274 | 0.595231 | 0.595259 | 0.595259 |
| 0.4 | 0.41 | 0.706338 | 0.706289 | 0.706321 | 0.706324 |
| | 0.44 | 0.710590 | 0.710543 | 0.710574 | 0.710576 |
| | 0.45 | 0.712011 | 0.711965 | 0.711995 | 0.711997 |
| | 0.46 | 0.713433 | 0.713388 | 0.713418 | 0.713419 |
| 0.6 | 0.41 | 0.791155 | 0.791114 | 0.791141 | 0.791143 |
| | 0.45 | 0.795717 | 0.795678 | 0.795704 | 0.795705 |
| | 0.5 | 0.801463 | 0.801427 | 0.801450 | 0.801451 |
| | 0.53 | 0.804921 | 0.804888 | 0.804910 | 0.804910 |
| 1 | 0.41 | 0.937285 | 0.937255 | 0.937275 | 0.937277 |
| | 0.45 | 0.940574 | 0.940545 | 0.940564 | 0.940565 |
| | 0.58 | 0.951406 | 0.951384 | 0.951398 | 0.951398 |
| | 0.6 | 0.953076 | 0.953056 | 0.953069 | 0.953069 |

Table 7: Values of $-\phi'(0)$ for various Rc, A when $Gr = Gc = 0.1$, $M = 0.5$, $Sc = 0.62$ $Rd = 0.5$ and $\Pr = 6.2$:

| Sc | A | $-\phi'(0)$ | | | |
|---|---|---|---|---|---|
| | | $Cu$ | $Ag$ | $Al_2O_3$ | $TiO_2$ |
| 0.5 | 0.41 | 0.667016 | 0.666975 | 0.667002 | 0.667004 |
| | 0.45 | 0.671874 | 0.671835 | 0.671861 | 0.671862 |
| | 0.5 | 0.678017 | 0.677981 | 0.678004 | 0.678005 |
| | 0.6 | 0.690399 | 0.690373 | 0.690390 | 0.690390 |
| 1 | 0.41 | 0.970785 | 0.970734 | 0.970768 | 0.970771 |
| | 0.44 | 0.974836 | 0.974786 | 0.974819 | 0.974821 |
| | 0.45 | 0.976185 | 0.976136 | 0.976168 | 0.976170 |
| | 0.46 | 0.977532 | 0.977484 | 0.977516 | 0.977518 |
| 1.8 | 0.41 | 1.327096 | 1.327037 | 1.327076 | 1.327079 |
| | 0.45 | 1.332757 | 1.332702 | 1.332738 | 1.332741 |
| | 0.5 | 1.339749 | 1.339699 | 1.339732 | 1.339733 |
| | 0.53 | 1.343890 | 1.343844 | 1.343874 | 1.343875 |
| 4 | 0.41 | 2.015285 | 2.015220 | 2.015263 | 2.015266 |
| | 0.45 | 2.021111 | 2.021050 | 2.021090 | 2.021093 |
| | 0.58 | 2.039374 | 2.039331 | 2.039359 | 2.039359 |
| | 0.6 | 2.042078 | 2.042038 | 2.042064 | 2.042064 |

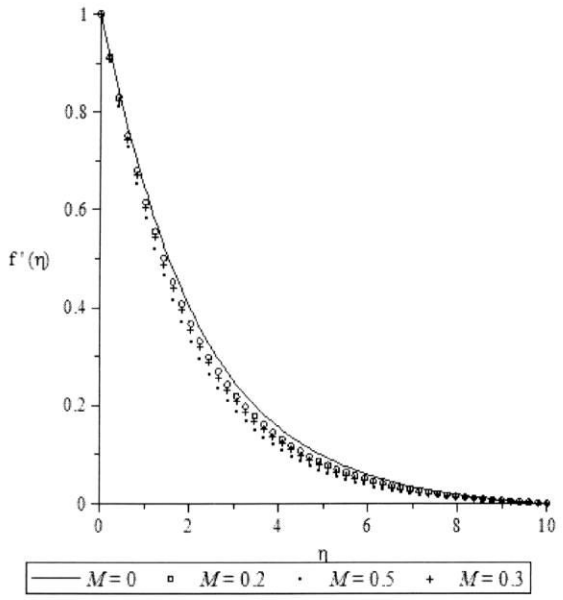


Fig. 2: Effect of M on velocity distribution $F'(\eta)$ for Pr = 6.2 and $\mathrm{A} = 0.5$

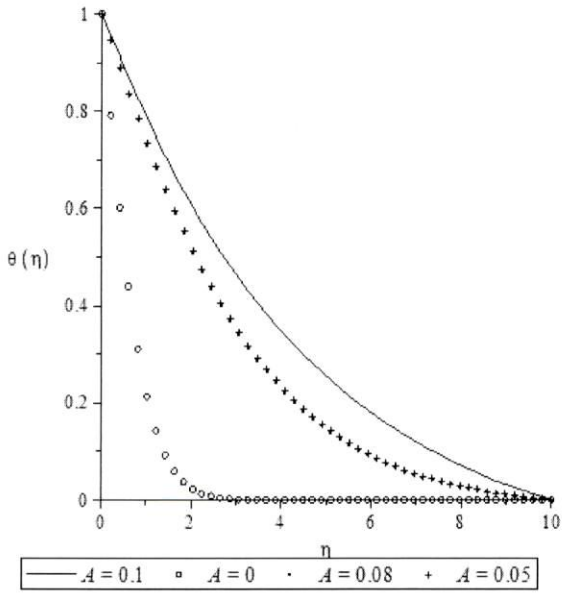


Fig.3: Effect of A on temperature distribution $\theta(\eta)$ for Pr = 6.2 and $M = 0.5$

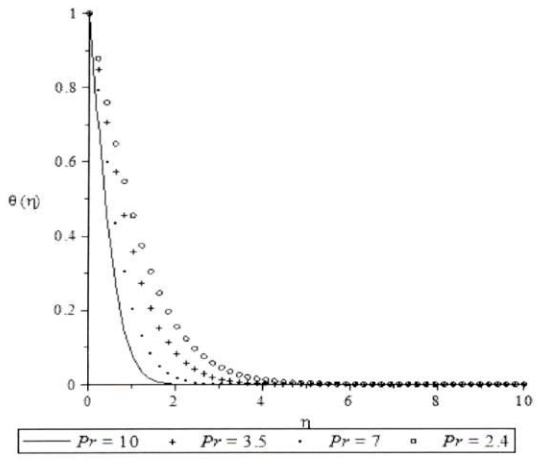


Fig.4: Effect of Pr on temperature distribution $\theta(\eta)$ for $R_d = 0.5$ and $\mathrm{A} = 0.5$

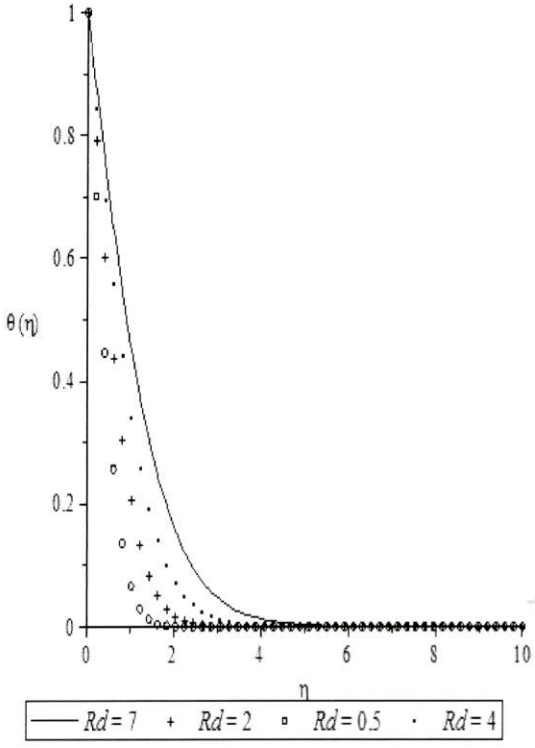


Fig5: Effect of Rd on temperature distribution $\theta(\eta)$ for Pr = 6.2 and $M = 0.5$

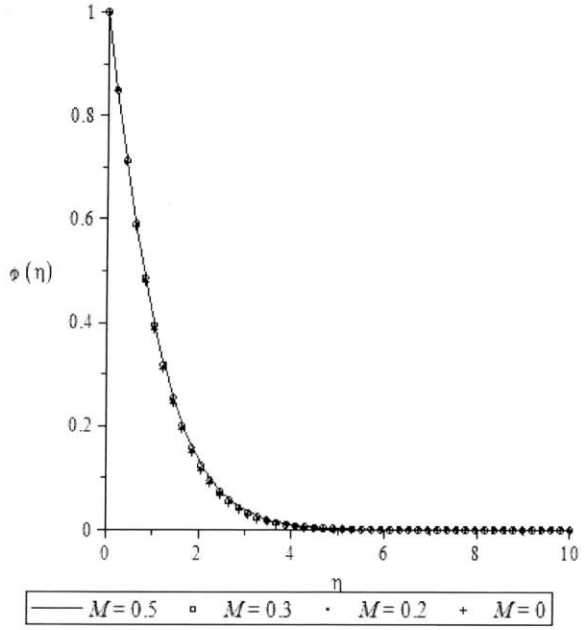


Fig.6: Effect of M on concentration distribution $\phi(\eta)$ for Pr = 6.2 and $A = 0.5$

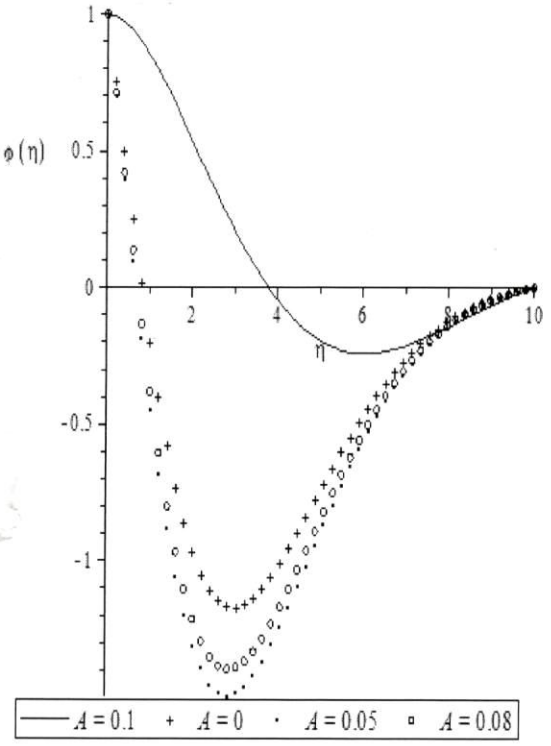


Fig.7: Effect of A on species concentration distribution $\phi(\eta)$ for Pr = 6.2 and $Rc = 0.5$

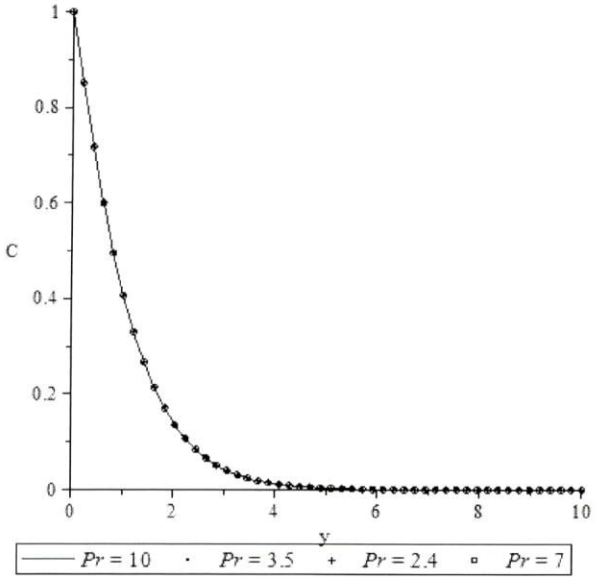


Fig.8: Effect of Pr on species concentration distribution $\phi(\eta)$ for $R_d = 0.5$ and $A = 0.5$

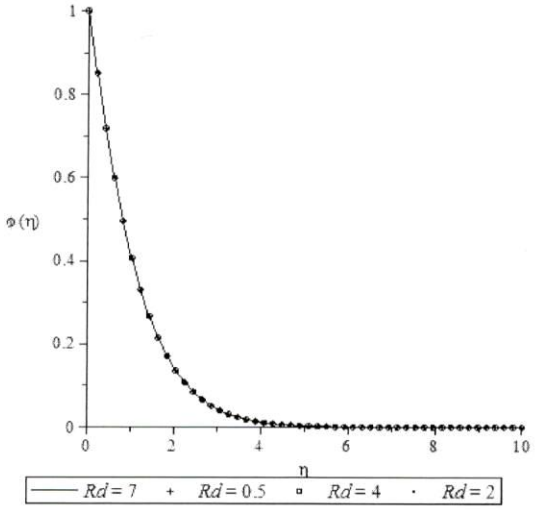


Fig.9: Effect of $Rd$ on species concentration distribution $\phi(\eta)$ for $\Pr = 6.2$ and $A = 0.5$

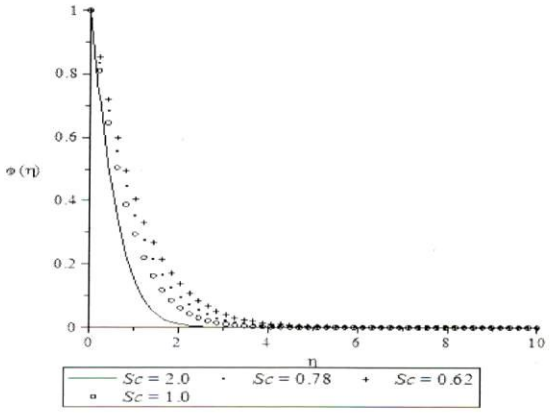

Fig.10: Effect of $Sc$ on species concentration distribution $\phi(\eta)$ for $\Pr = 6.2$ and $Rc = 0.5$

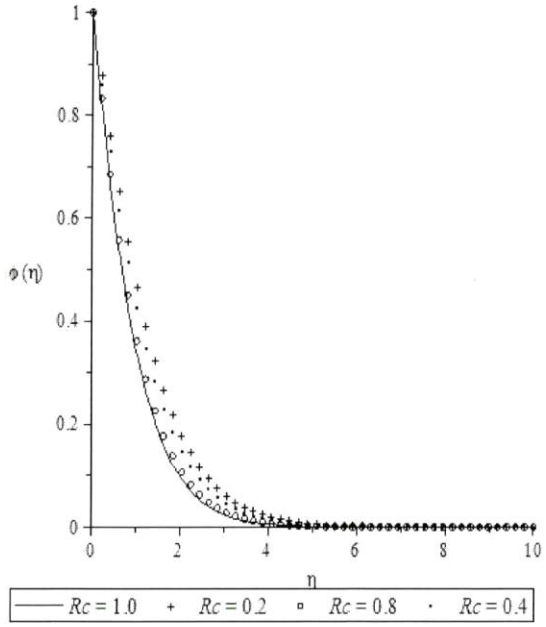


Fig.11: Effect of $Rc$ on species concentration distribution $\phi(\eta)$ for $\Pr = 6.2$ and A = 0.5

## 5.0 DISCUSSION OF RESULTS

The influences of various thermophysical parameters on the velocity, temperature and species concentration distributions are described in this section. It is partinent to note that the magnetic parameter M, nanoparticle volume fraction A, Prandtl number Pr, Thermal radiation $R_d$, Schmidt number Sc and the rate of chemical reaction parameter $R_c$ have significant effects on the dimensionless velocity, temperature and species concentration distributions. These are shown in figures 2 – 11. Physical quantity of engineering interests here are the Skin friction coefficient ($C_f$), the Nusselt number (Nu) and the Sherwood number (Sh). From derivations, these can be written as follows;

$$C_f = -f''(0);\ \text{Nu} = -\theta'(0) \text{ and Sh} = -\phi'(0)$$

**Velocity Distribution:** Figure 2 depicts the velocity profile for various values of the magnetic field parameter in the case of Cu-Water when A = 0.5. We observe that the velocity along the surface decreases as the magnetic field parameter increases. This shows that the Lorentz force is responsible for the opposition to the fluid motion. Hence, the presence of the magnetic field decreases the momentum boundary layer thickness.

**Temperature Distribution:**Fig. 3 shows that at lower values, the solid volume fraction of the nanoparticle, has no effect on the temperature distribution. However, at higher values of the nanoparticle volume fraction, the temperature distribution is found to decrease. Fig.4 shows that as the Prandtl number increases, temperature distribution decreases. Figure 5 shows the effect of the thermal radiation Rd on the temperarturedistribution. It is observed that the rate of heat transfer increases with the increase in the thermal radiation parameter. Hence, high effect of thermal radiation enhances high rate of heat transfer .

**Concentration Distribution:** In Figures 6 – 11, the effects of the Magnetic parameter, nanoparticles volume fraction, radiation and chemical reaction parameters, Schmidt and Prandtl numbers on the species concentration are displayed. We observed in Fig. 6 that increase in the magnetic parameters results in increase in the concentration distribution . In Fig. 7, we see that a decrease in the solid volume fraction (A), leads to a decrease in the concentration $\phi(\eta)$ but with a minimum value along the profile. In Fig. 8, we see that increase in the Prandtl number leads to slight decrease in the concentration distribution. Slight decreases in the concentration are also observed from Fig. 9 when the radiation parameter decreases. A look at Fig. 10 shows that the Schmidt number has a pronounced significant effect on the concentration distribution as a reduction in the Schmidt numbers leads to an increase in the concentration. In Fig. 11, we see the effect of the chemical reaction parameter being displayed. Here, it is observed that, increase in chemical reaction parameter increases the concentration of the nanofluid.

Results from the tables show and confirm the effects of the magnetic parameters, the particle volume fraction, Schmidt numbers, radiation parameter and the chemical reaction parameter on the velocity, temperature and concentration distributions as earlier observed from the figures.

Table 2 shows that as the magnetic parameter increases, the velocity profile decreases. This means that the skin friction increases with an increase in the magnetic parameter. This result is in agreement with what was obtained in fig. 2. It is further observed that at the same values of the magnetic parameter and the particle volume fraction (e.g. A = 0.41 and M = 0), the skin friction of copper is less than those of Silver, Aluminium oxide and Titanium oxide.

Table 3 shows the effect of the radiation parameter and the particle volume fraction on the temperature distribution. When the radiation parameter is increased, it increases the temperature distribution while an increase in the particle volume fraction decreases the temperature profile.

Table 4 shows the effect of the magnetic parameter and the solid volume fraction on the concentration distribution. As the magnetic parameter is increased, concentration profile also increases. Similarly, increase in the particle volume fraction has an increasing effect on the concentration distribution. However, at very high value of the magnetic parameter, concentration profile decreases. Concentration profile is higher in silver than either Copper, Alumina or Titanium oxide.

Table 5 shows that increase in the radiation parameter has a decreasing effect on the concentration profile while an increase in the particle volume fraction has an increasing effect on the concentration profile of the nanofluid. The Sherwood number increases as both the radiation parameter and the solid volume fraction increases.

In table 6, we also see that the Schimidt number has an inceasing effect on the concentration profile of the nanofluid while in table 7 the chemical reaction is seen to have an increasing effect on the nanofluid.

## 6 CONCLUSIONS

We have investigated the effect of chemical reaction and thermal radiation on the convective flow, heat and mass transfer of an incompressible viscous nanofluid past a semi-infinite vertical stretching sheet. The governing partial differential equations with the boundary conditions were reduced to ordinary differential equations with the appropriate corresponding conditions using non-dimensional quantities and the resulting differential equations were solved numerically using the Runge - Kutta – Fehlberg method.

The presented analysis has shown that the nanoparticle volume fraction, magnetic field parameter and other thermophysical parameters appreciably influence the velocity, temperature and species concentration distributions. We therefore make the following conclusions:

- The magnetic parameter has decreasing effects on the velocity but an increasing effect on the species concentration distribution.
- Increase in the nanoparticle volume fraction parameter decreases the temperature but increases the species concentration fields.
- As the Schmidt number decreases, there is a significant increase in the species concentration profile.
- The temperature and species concentration distributions increase as the thermal radiation parameter increases but they decrease as the Prandtl number increases.
- The chemical reaction parameter has a significant increasing effect on the species concentration.

## REFERENCES


[1] Alloui Z., Vasseur P., Reggio M. (2012); Analytical and numerical study of bouyancy-driven convection in a vertical enlosure filled with nanofluids. J Heat and Mass Transfer 2012 48; 627-629.

[2] FakhreddineSegniOueslati, RachidBennaccer. (2011); Heterogeneous Nanofluids Natural Convection Heat Transfer Enhancement.Nanoscale ResearchLetters.Vol6(1), : 222 http/www.nanocaslett.com/content/6/1/222. Nanofluid models.

[3] Godson, L., Raja B, Mohan Lal D and Wongwises S. (2010); Enhancement of Heat Transfer Using nanofluids; An overview, Renewable and Sustainable energy Reviews. Vol.14, pp 629 – 641.

[4] Hamad M. A. A. (2011); Analytical Solution of Natural convection flow of a Nanofluids over a linearly stretching sheet in the presence of magnetic field. International Communications in Heat and Mass Transfer; 38, 487 – 492

[5] Kakac S, Pramuanjaroenkij A. (2009); Review of Convective Heat Transfer Enhancement with nanofluids, Int. J. Heat and Mass Transfer. 52 (2009), pp 3187 – 3196.

[6] Khan, W.A.and I. Pop (2010); Boundary- Layer flow of a nanofluid past a streching sheet. International Journal of Heat and Mass Transfer 53(2010), 2477-2483.

[7] Kuznetsov A. V, Nield D. A. (2010); Natural Convective Boundary-Layer flow of a nanofluid past a vertical plate; Int. J. Thermal Sci. 49, 247 – 257

[8] KyuHyung Do, Soek, Pill Jang (2010); Effect of nanofluids on the thermal performance of a flat micro heat pipe with a rectangular grooved wick; Inter. Journal of Heat and Mass Transfer. 53 (2010) 2183 – 2192.

[9] Ozerinc S, Kakac S, and Yazicioglu. (2010); Enhanced Thermal Conductivity of Nanofluids a "state-of-the-art review".Microfluidics and nanofluidics, vol. 8, pp 145 – 175.

[10] P. K. Sarma, C.Kedarnath, C. P. Ramanarayanan, P. S. Kishore, V. Dharma Rao, K.Ramakrishna, and V.Srinivas (2008), Turbulent Convective Heat Transfer Characteristics Of Nano Fluid In A Circular Tube, International Journal of Heat and Technology, Vol. 26 (2), 85 – 93.

[11] P.K.Sarma, KedarnathChada, K.V. Sharma, L. Shyam Sundar, P.S. Kishore, V.Srinivas (2010) Experimental Study To Predict Momentum And Thermal Diffusivities From Convective Heat Transfer Data Of Nano Fluid With Al2o3 Dispersion, International Journal of Heat and Technology, Vol. 28 (1),123 -137.

[12] Wang X.Q and Mujumdar A.S (2007); Heat transfer characteristics of nanofluids: A review, International Journal of Thermal Sciences 46, 1-19.

[13] Sidi El BécayeMaïga, Samy Joseph Palm,Cong Tam Nguyen,Gilles Roy and Nicolas Galanis (2005), Heat transfer enhancement by using nanofluids in forced convection flows, International Journal of Heat and Fluid Flow, vol. 26 (4), 530–546.

[14] Zaimi, K., Ishak, A. & Pop, I. (2014), Boundary layer flow and heat transfer over a nonlinearly permeable stretching/shrinking sheet in a nanofluid. Sci. Rep. 4, 4404;DOI:10.1038/srep04404 (2014).

[15] Md. Shakhaoath Khan1*, Ifsana Karim1 and Md. Sirajul Islam (2014) Possessions of Chemical Reaction on MHD Heat and Mass Transfer Nanofluid Flow on a Continuously Moving Surface, American Chemical Science Journal, 4(3): 401-415.

[16] A. Rasekh and D.D. Ganji and S. Tavakoli, (2012, Numericalsolution for a nanofluid past over a stretching Circularcylinder with non-unifom heat source, Frontiers Heat. Mass.Transf. (FHMT), 3, 043003.

[17] AminrezaNoghrehabadi*, Mohammad Ghalambaz, EhsanIzadpanahi, Rashid Pourrajab (2014), Effect of magnetic field on the boundary layer flow, heat, and mass transfer of nanofluids over a stretching cylinder, Journal of Heat and Mass Transfer Research 1 9-16.